Selectively Scissoring Hydrogen-Bonded Cytosine Dimer Structures Catalyzed by Water Molecules

Lei Xie,[▽] Huijun Jiang,[▽] Donglin Li,[▽] Mengxi Liu,[▽] Yuanqi Ding, Yufang Liu, Xin Li, Xuechao Li, Haiming Zhang, Zhonghuai Hou, Yi Luo, Lifeng Chi,* Xiaohui Qiu,* and Wei Xu*

Cite This: *ACS Nano* 2020, 14, 10680−10687

Read Online

ACCESS | 📊 Metrics & More | 📄 Article Recommendations | 🆘 Supporting Information

ABSTRACT: A single-molecule-level understanding of the activity of solvating water molecules in hydrogen-bonded assemblies would provide insights into the properties of the first hydration shells. Herein, we investigate the solvation of one of the DNA bases, cytosine, whose glassy-state network formed on Au(111) contains diverse types of hydrogen-bonded dimer configurations with hierarchical strengths. Upon water exposure, a global structural transformation from interwoven chain segments to extended chains was identified by scanning tunneling microscopy and atomic force microscopy. Density functional theory calculation and coarse-grained molecular dynamics simulation indicate that water molecules selectively break the weak-hydrogen-bonded dimers at T-junctions, while the stable ones within chains remain intact. The resulting hydrated chain segments further self-assemble into molecular chains by forming strong hydrogen bonds and spontaneously releasing water molecules. Such an intriguing transformation cannot be realized by thermal annealing, indicating the dynamic nature of water molecules in the regulation of hydrogen bonds in a catalytic manner.

KEYWORDS: *hydrogen bond regulation, water catalysis, scanning tunneling microscopy, atomic force microscopy, dynamics simulation*
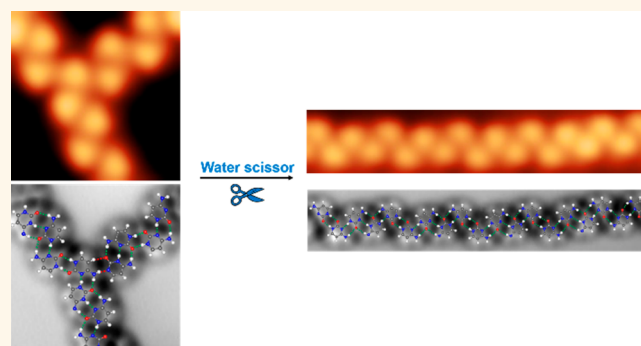
S elf-assembly plays a vital role in numerous biological processes pertaining to specific biomacromolecules, *e.g.*, DNA double-helix structure and high-fidelity replication, protein folding, formation of a ribosome and phospholipid bilayer, *etc.*, which maintains cellular life.[1,2] Such sophisticated self-assembled structures are normally associated with the cooperation and competition of various noncovalent interactions,[3] involving but not limited to hydrogen bonding,[4] coordination bonding,[5,6] electrostatic ionic bonding,[7] and van der Waals interactions.[8] Thus, detection and further regulation of these noncovalent interactions within hierarchically self-assembled structures is important for understanding the fundamental mechanism in biological self-assembly processes. As is known, water is one of the most important and indispensable small molecules *in vivo*,[9] which plays a crucial role in regulating functions and structures of biomolecules and further driving the biological self-assembly processes. The interactions between water and biomolecules have been studied in detail by a range of techniques. For instance, X-ray and neutron diffraction can provide time-averaged equilibrium structures of hydrated molecules in crystalline

and disordered states.[10,11] Information of the dynamical structure of hydrogen-bonded networks is often obtained by NMR and time-resolved infrared spectroscopy.[12] However, the inhomogeneity of the systems still poses a tremendous challenge to these ensemble-averaged measurements. The lack of spatial specificity hampers further elucidation of intermolecular structural correlation. A single-molecule-level understanding of how solvating water molecules mediates intermolecular hydrogen bonds and transforms the structures of molecular assemblies is still incomplete. On the other hand, high-resolution scanning probe microscopy has been employed to provide real-space structural information on water clusters and hydrated organic molecules.[13,14] Moreover, water
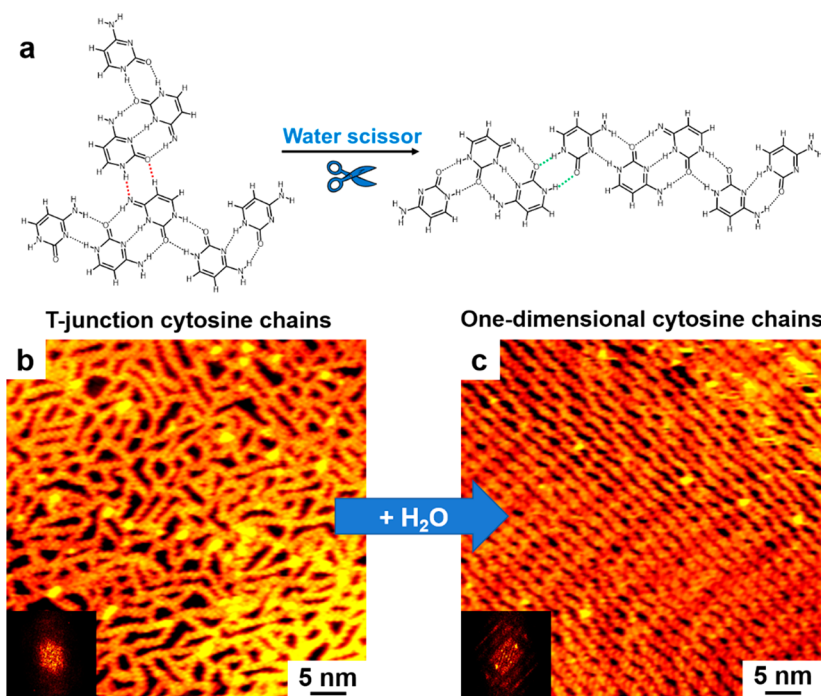
Figure 1. Overview of water-induced phase transition from T-junction cytosine chains to extended one-dimensional chains on Au(111). (a) Schematic illustration showing water molecules behaving as scissors selectively cut off the hydrogen-bonded dimer at the junction (depicted by red dashed lines), and the unperturbed chain segments self-assemble into extended chains by forming strong hydrogen bonds (depicted by green dashed lines). (b and c) Large-scale STM images and the corresponding FFT insets showing the water-induced structural transformation from cytosine chains linked by various T-junctions to extended chains in parallel on Au(111).

molecules were found to be able to perturb hydrogen bonds in a self-assembled molecular structure.[15]

In this study, we choose one of the DNA bases, the cytosine molecule, which forms a glassy-state molecular assembly on the Au(111) surface that resembles a two-dimensional fluid at room temperature and contains diverse types of hydrogen-bonded dimer configurations with hierarchical strengths.[16] Herein, using scanning tunneling microscopy (STM) and single-bond-resolved noncontact atomic force microscopy (nc-AFM) imaging, we demonstrate that upon water exposure, a global structural transformation from randomly interwoven molecular chain segments to densely packed extended chains surprisingly occurs. The connecting dimer structures at various T-junctions are broken, and the dimers constituting molecular chain segments remain intact under water perturbation, which further self-assemble into longer molecular chains (Figure 1a–c). The water-induced dynamics of hydrogen-bonded dimer structures and the consequent self-assembled structures is revealed by density functional theory (DFT) calculations and large-scale simulation of the assembly dynamics based on a coarse-grained model.

RESULTS AND DISCUSSION

A careful inspection of the disordered cytosine network indicates that it is composed of molecular chain segments of varying lengths randomly linked together by various T-junctions as shown in Figure 2a and b. The STM and nc-AFM images of two typical T-junction structures are shown in Figure 2c,d, 2f,g, respectively. The proposed structural models are superimposed on the enlarged nc-AFM images (Figure 2e and h). It is noted that only using the canonical form of cytosine cannot rationalize the observed structures and the accompanying hydrogen-bonding configurations determined

from nc-AFM images. As previously reported, tautomerization of DNA base molecules on surfaces is a universal phenomenon,[17−20] and cytosine tautomers have also been theoretically and experimentally verified.[21,22] Based on that, we involve another two tautomers of cytosine (cf. the inset of Table 1) in the proposed structural models. On the basis of the above information, we propose that molecular chain segments are composed of several characteristic hydrogen-bonded dimer configurations of dimer 1−8, and T-junctions (indicated by red arrows) are composed of hydrogen-bonded dimer configurations of dimer 9−14 (cf. Table 1 for the labeling).

After deposition of water molecules on such an interwoven network at room temperature, all of the T-junctions disappear and the extended molecular-chain array was observed as shown in the STM images of Figure 2i and j (larger-scale STM images of chains are shown in Figure S1). The FFT image shown in Figure 2i depicts a pronounced periodicity (16.5 ± 0.2 Å) with a specific direction corresponding to the distance between the chains, indicating a long-range ordering. An example of the one-dimensional chain is shown in Figure 2k−m, where the proposed structural model is superimposed on the enlarged nc-AFM image. We identify that the molecular chain is also composed of characteristic hydrogen-bonded dimer configurations of dimer 1−8, which is intrinsically the same as the chain segments before water deposition. More examples of proposed structural modeling assignments of T-junction chains and extended chains are also illustrated in Figure S2.

In order to understand the mechanism of water-induced rearrangement of cytosine assemblies, we carry out extensive DFT calculations by comparing each individual hydrogen-bonding energy between the water-involved hydrogen bonds (formed in hydrated cytosine) and the original ones formed in the corresponding dimer structures. As shown in the upper

T-junction cytosine chains

One-dimensional cytosine chains
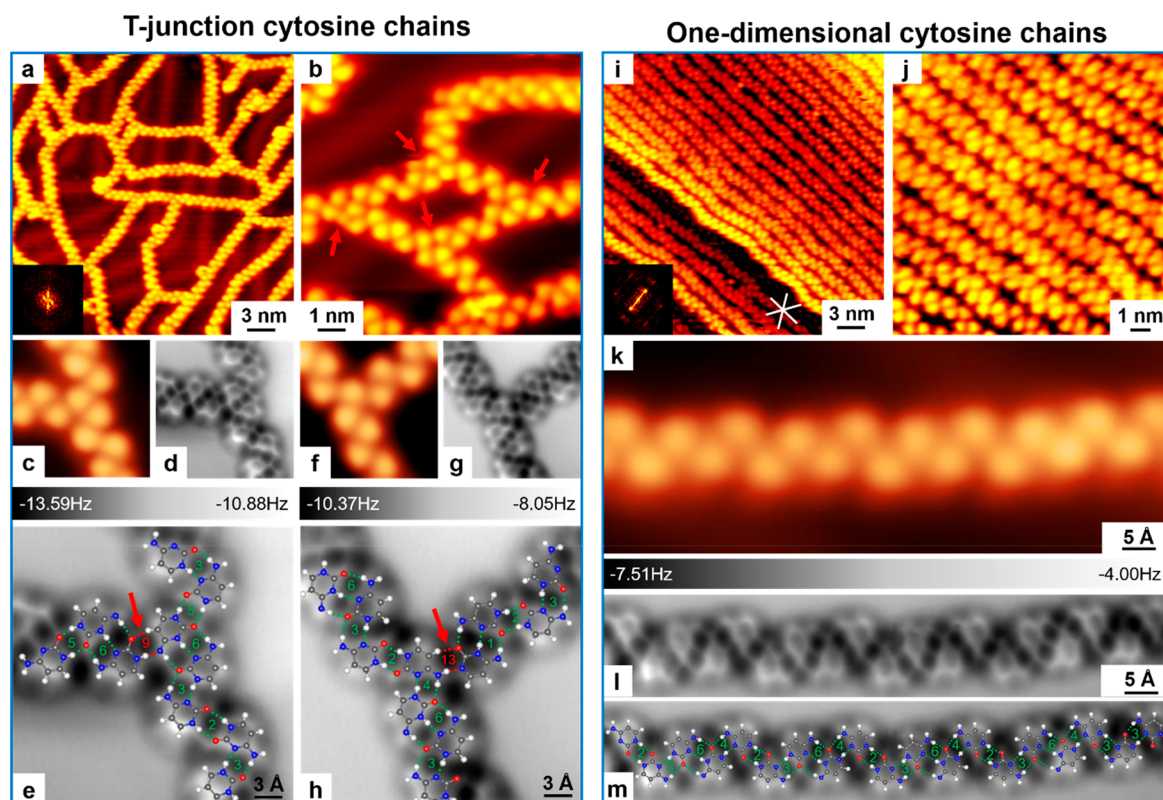
Figure 2. STM and single-bond-resolved nc-AFM images of T-junction cytosine chains (left panel) and one-dimensional cytosine chains (right panel) with proposed models superimposed. (a) Large-scale STM image of cytosine chains linked by various T-junctions on Au(111). (b) Close-up STM image showing the randomly existing T-junctions indicated by red arrows. (c, d) High-resolution STM image and the corresponding single-bond-resolved nc-AFM image of a typical T-junction structure, respectively. (e) Enlarged nc-AFM image with a proposed model in which weak hydrogen bonds (depicted by red dashed lines) form the fragile dimer 9 (*cf.* Table 1) at the junction and strong hydrogen bonds (depicted by green dashed lines) form various stable dimer configurations of dimer 1−dimer 8 (*cf.* Table 1) within the chains. (f, g, h) High-resolution STM image and the corresponding nc-AFM image of another T-junction structure, respectively. The enlarged nc-AFM image with a proposed model showing the formation of the fragile dimer 13 at the junction and stable dimer configurations within the chains. (i, j) Large-scale and close-up STM images of water-induced formation of extended one-dimensional parallel chains on Au(111). (k, l, m) High-resolution STM image and the corresponding nc-AFM image of an extended chain structure, respectively. The nc-AFM image with a proposed model showing the chain is also composed of stable dimer configurations of dimer 1−dimer 8 (*cf.* Table 1). Structural model: H: white, C: gray, N: blue, O: red.
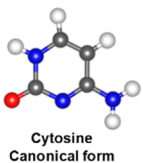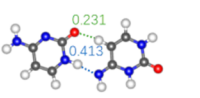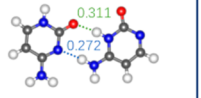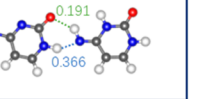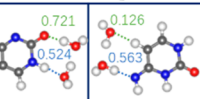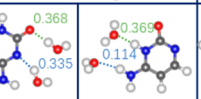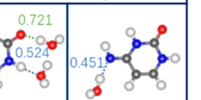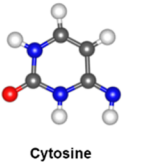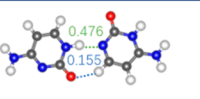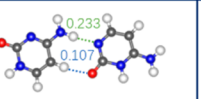
panel in Table 1, all of the hydrogen bonds within the dimer 9−14 at T-junctions are weaker than the corresponding water-involved hydrogen bonds of at least one hydrated cytosine molecule displayed beneath the dimers; thus these fragile dimers are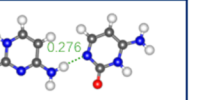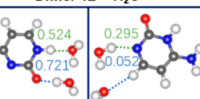 easily broken by water molecules from an energy point of view. In the lower panel, for the dimer 1−8 in molecular chains, at least one individual hydrogen bond within each dimer is stronger than the corresponding water-involved hydrogen bonds of both hydrated cytosine molecules, which reveals that those dimers are stable and preserved under water perturbation.

To further understand the process of this unexpected water-induced structural transformation, a coarse-grained model is proposed for simulation of large-scale collective dynamics of cytosine molecules. Figure 3a−d show the simulated growth process of the cytosine self-assembled structure from individual molecules to T-junction chains (also see Movie S1). After introducing water into the system, the number of T-junctions gradually decreases and the growth of extended one-dimensional chains prevails, as shown in Figure 3e−h (also see Movie S2). Details of this process are elaborated in the snapshot images at different stages in chronological order (Figure 3i−k and Movie S3).
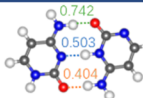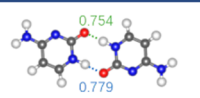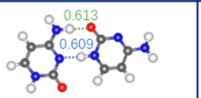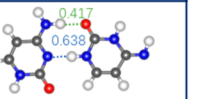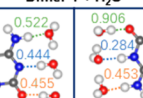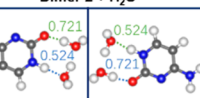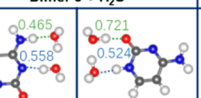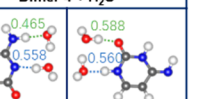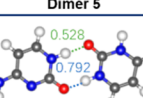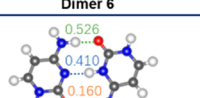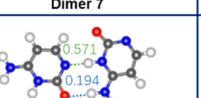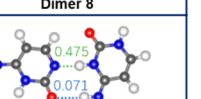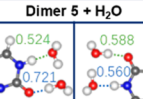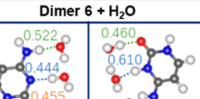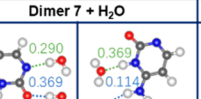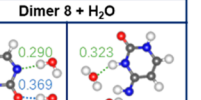
The whole process can be presented as follows: (i) Cytosine molecules self-assemble into the glassy-state structure on the Au(111) surface where both strong and weak hydrogen bonds are formed as depicted by green and red dots, respectively (Figure 3i); (ii) water molecules detect all of the possible intermolecular hydrogen bonds formed in the structure and are inclined to bind to all of the feasible sites of cytosine molecules, and as a result, weak hydrogen bonds at T-junctions are selectively broken (*cf.* Table 1); meanwhile stronger water-involved hydrogen bonds are formed as depicted by blue dots (Figure 3j); (iii) the molecular chain segments (binding with water molecules at terminals) are unable to form T-junctions again. In the next step, they diffuse as supermolecules on the surface and further self-assemble into longer molecular chains in an end-to-end manner provided that strong hydrogen bonds are formed (*cf.* Table 1) (meanwhile, water molecules are released), resembling the game "Gluttonous Snake" (Figure 3k). Thereafter, water molecules desorb from the Au(111) surface owing to the low adsorption energy.[23,24] (iv) Moreover, the peripheral hydrogen atoms of molecules make chains laterally arranged *via* van der Waals interactions, resulting in a close-packed array.

Table 1. DFT Calculations on Various Hydrogen-Bonded Cytosine Dimers Formed at Junctions and in Chains and the Corresponding Hydrated Cytosine, Together with Each Individual Hydrogen-Bonding Energy[a]

[a]Inset: three cytosine tautomers involved: canonical form, tautomer 1, and tautomer 2. Upper panel: the fragile dimers 9−14 formed at various T-junctions composed of relatively weak hydrogen bonds, which are easily broken by water. Lower panel: the stable dimers 1−8 formed in chains composed of relatively strong hydrogen bonds, which cannot be broken by water. The corresponding hydrated cytosine with water-involved hydrogen bonds using the same interaction sites is displayed beneath each dimer. The calculated energy values (eV) of each individual hydrogen bond are listed nearby.

Note that such a structural transition cannot be realized by a normal annealing treatment (cf. Figure S3). We thus propose that annealing the sample (globally) to a certain temperature results in the overall breakage of both strong and weak hydrogen bonds without a precise selectivity. On the other hand, as shown above, water molecules may efficiently detect all of the hydrogen bonds in a very localized manner, i.e., at the single-bond level. Meanwhile, the water molecule provides a catalyzed pathway that reduces the activation energy barrier for the hydrogen-bonding breakage by forming water-involved hydrogen bonds, facilitating the conversion of intermolecular hydrogen-bonding configurations to the thermodynamically more favorable states, and no structural transformation would happen after further thermal treatment.

CONCLUSIONS

In conclusion, from a combination of high-resolution STM and nc-AFM imaging, DFT calculation, and large-scale molecular dynamics simulation, we demonstrate that water molecules are able to effectively regulate self-assembled structures of cytosine by precisely manipulating individual hydrogen bonds in a catalytic manner. Water molecules discussed in this case are mediators that selectively break the weak hydrogen bonds by forming moderate ones in hydrated species, and the latter are displaced when stronger intermolecular hydrogen bonds are formed and thereafter desorb from the surface, behaving as a catalyst in the overall structural transformation process. We believe that the present results give a clear example of water molecules in regulating intermolecular hydrogen bonds in a hierarchical self-assembled system. The real-space information

Simulated growth process of cytosine chains with T-junctions

(a) H_2O off, time=0 (b) H_2O off, time=1000 (c) H_2O off, time=5000 (d) H_2O off, time=11990

+ H_2O

Simulated growth process of cytosine 1-D chains induced by water

(e) H_2O on, time=12000 (f) H_2O on, time=13990 (g) H_2O on, time=16990 (h) H_2O on, time=130990

T-junction chains
Strong and weak HB

Weak HB breakage
Water-involved HB formation

Strong HB formation
Squeezing off water

(i) H_2O off, time=11990 (j) H_2O on, time=12480 (k) H_2O on, time=13200

Figure 3. Dynamics simulations of the growth process of cytosine chains linked by various T-junctions and the water-induced transition from T-junction chains to extended one-dimensional chains on the surface. (a−d) Simulated growth process of T-junction cytosine chains. (e−h) Simulated growth process of extended 1-D cytosine chains induced by water. (i−k) Series of zoomed-in simulated images of one spot in chronological order showing the details: (i) the formation of cytosine chains (*via* strong hydrogen bonds) linked by T-junctions (*via* weak hydrogen bonds) (indicated by a red arrow), (j) the breakage of weak hydrogen bonds and meanwhile the formation of water-involved hydrogen bonds (indicated by blue arrows), and (k) the re-formation of strong hydrogen bonds (indicated by green arrows) by releasing the water molecules. Cytosine molecules are presented as unicolor species in light or dark green representing R or L chirality, respectively. Green dots: strong hydrogen bonds; red dots: weak hydrogen bonds; blue dots: water-involved hydrogen bonds. Time is displayed in arbitrary units.

at the single-bond level would be complementary to time-resolved measurements and further improves our understanding of the dynamic interfaces between biomolecules and incorporated water molecules.

METHODS

STM/nc-AFM Measurements. Experiments were carried out in two independent ultra-high-vacuum (UHV) systems that host a SPECS variable-temperature "Aarhus-type"[25,26] and a low-temperature Omicron scanning tunneling microscope, respectively, where the base pressure was ∼1 × 10⁻¹⁰ mbar. The Au(111) substrate was prepared by several cycles of 1.5 keV Ar⁺ sputtering followed by annealing to 800 K for 10 min, resulting in clean and flat terraces separated by monatomic steps. The cytosine molecules (purchased from Sigma-Aldrich, purity >98%) were loaded into a glass crucible in the molecular evaporator. The pure deionized water (purchased from Sigma-Aldrich) was loaded in a dosing tube positioned in the preparation chamber and further purified under vacuum by several freeze−thaw cycles to remove the remaining impurities.[27] After a thorough degassing, cytosine molecules were deposited onto the

Au(111) substrate by thermal sublimation at 370 K, and water molecules were dosed onto the surface held at room temperature at a pressure of 1 × 10⁻⁵ mbar for 1 min; the sample was thereafter transferred within the UHV chamber to the STM, where measurements were carried out at ∼100−150 K. Scanning conditions: I_t = 0.5−0.9 nA, V_t = −1700 mV. All of the STM images were further smoothed to eliminate noise. For the experiments performed in the Omicron system, the STM images were taken in the constant-current mode and the voltage was applied on the sample while the tip was grounded. The nc-AFM measurement was carried out at liquid helium temperature in constant-height frequency modulation mode with a CO-functionalized tip (resonance frequency f_0 = 42.15 kHz, oscillation amplitude A = 170 pm, quality factor Q = 8 × 10⁴).

Theoretical Calculations. As the interaction between molecules and the Au(111) surface is relatively weak as proved by the integrity of the herringbone reconstruction, we then perform the following calculations in the gas phase. The calculations were performed in the framework of DFT by using the Vienna *ab initio* simulation package (VASP).[28,29] The projector-augmented wave method was used to describe the interaction between ions and electrons;[30,31] the Perdew−Burke−Ernzerhof generalized gradient approximation (GGA) ex-

change−correlation functional was employed;[32] and the dispersion-corrected DFT-D3 method of Grimme[33] was used for the calculations when including the weak interactions. The atomic structures were relaxed using the conjugate gradient algorithm scheme as implemented in the VASP code until the forces on all unconstrained atoms were ≤0.03 eV/Å. Based on the optimized hydrogen-bonded dimer configurations, the dispersion-corrected DFT-D3 was used to calculate the single-point energy by the Gaussian 16 program package.[34] The single-point energies were calculated at the M06-2X-D3/6-311++G(d,p) level, which incorporates dispersion and long-range corrections.[35,36] Multiwfn 3.2.1 was used to perform wave function analysis and calculate the intermolecular hydrogen-bonding energy.[37]

To facilitate the large-scale simulation of the assembly process for cytosine molecules without and with water, we proposed a coarse-grained model where the cytosine molecules (including the canonical form and two tautomers) are considered to be a rigid body (taking the canonical form as an example) consisting of beads located at positions of the contained atoms as illustrated in Figure S4. These beads represent binding sites of possible hydrogen bonds listed in Table 1. Due to the nonsymmetrical distribution of the hydrogen donor and acceptor groups (*i.e.*, the corresponding hydrogen bond binding sites) over the periphery of the cytosine molecule, we assign site 1, site 2, and site 3 to strong hydrogen bond binding sites (annotated as S1, S2, and S3) and S4, S5, and S6 to weak hydrogen bond binding sites. Then, the relevant sites of each molecule involved in hydrogen bonds will be indicated explicitly as, e.g., S1S1, *etc.* Moreover, the sites of cytosine molecules with different chiralities are denoted as S and $\overline{S}$ for clarity (*cf.* Figure S4).[38]

As the hydrogen bonds are much weaker than covalent bonds, the assembly processes should be attributed to the intermolecular movement due to the hydrogen-bonding interactions and other weak intermolecular interactions rather than the inner-molecule movement. This allows us to describe the translational and the rotational motions of a rigid cytosine molecule with exclusive volume effects by

$$\gamma \dot{\mathbf{R}}_i = -\sum_j \frac{\partial}{\partial r_j} U_{tot} + \xi(t) \tag{1}$$

$$\gamma_\theta \dot{\theta}_i = -\sum_j \Gamma_j + \eta(t) \tag{2}$$

where $\mathbf{R}_i$ and θ_i denote the position and the rotating angle of the *i*th molecule, respectively, γ and γ_θ are the translational and rotational friction coefficients, and U_{tot} is the total interaction potential of the system, which leads to a force $-\frac{\partial}{\partial r_j} U_{tot}$ and a torque Γ_j exerting on the bead located at r_j in the molecule. Besides, both the translational and rotational motions suffer from Gaussian white noise due to the finite temperature, which reads $\xi(t)$ and $\eta(t)$, respectively. To be specific, the total interaction potential of the system includes hydrogen bond interaction potentials U_{HB} and effective exclusive volume potentials U_{EV}. The effective exclusive volume potentials are

$$U_{EV}(r_{ij}) = \begin{cases} 4\varepsilon \left(\dfrac{\sigma^{12}}{r_{ij}^{12}} - \dfrac{\sigma^6}{r_{ij}^6} \right), & r_{ij} < \sqrt[6]{2}\,\sigma \\ 0, & \text{otherwise} \end{cases} \tag{3}$$

where r_{ij} is the distance between any pair of beads and ε and σ are the effective strength and repulsive length, respectively. As we aim to understand qualitatively the effect of the hydrogen bond with water on the assembly process of cytosine molecules, the relative strengths of hydrogen bonds are important, which allows us to describe the hydrogen bond interaction potentials in the simplest manner with the relative strengths ensured to facilitate the large-scale simulation of the whole assembly process, *i.e.*,

$$U_{HB}(r_{ij}) = k_q (r_{ij} - R_{0,q})^2 \tag{4}$$

where r_{ij} is the distance between two sites that form a hydrogen bond and k_q and $R_{0,q}$ are the strength and the length of the hydrogen bond of type q, respectively. By defining a characteristic length l_0, a hydrogen bond is considered to be formed if $r_{ij} \leq l_0$ and to be broken if $r_{ij} > l_0$. There are also other hydrogen bond models in conventional molecular dynamics,[39−41] which describe accurately the intermolecular interaction accompanied by inner-molecular changes. The coarse-grained model should be further developed in the future if some quantitative accuracies need to be ensured. When water was introduced into the system, a hydrogen bond with a water molecule will be formed with a probability taking into account the collision frequency $p = cP_{H_2O}$ if the energy change is negative, where P_{H_2O} is the partial pressure of water and c is the coefficient. In simulations, $R_{0,q}$, γ, and $k_B T$ were set to be basic units for dimensionless, where k_B is the Boltzmann constant and T is the temperature. A total of 2500 molecules consisting of an equal number of L and R type ones were placed randomly on the metal surface with size 290×290 and periodic boundary conditions. Other parameters $\varepsilon = 200$, $\sigma = 1$, $l_0 = 1.5$, $\gamma_\theta = 9$, $c = 10^4$, and $P_{H_2O} = 10^{-5}$ mbar were the same as that in experiments. k_q for the hydrogen bond formed by S1S1 is set to be 150, and others take values that keep the same ratio relative to the S1S1 bond according to the DFT-calculated results shown in Table 1.

ASSOCIATED CONTENT

Ⓢ Supporting Information

The Supporting Information is available free of charge at https://pubs.acs.org/doi/10.1021/acsnano.0c05227.

Larger-scale STM images showing the formation of extended cytosine chains; nc-AFM images of more examples of T-junctions and extended chains; STM image of cytosine-precovered surface after annealing at 400 K; chemical structures of cytosine molecule and corresponding coarse-grained models (PDF)

Simulated growth process of cytosine chains with T-junctions (MP4)

Simulated transition process from T-junction chains to extended parallel chains induced by water (MP4)

Zoomed-in spot of the simulated growth process in Movie S2 during a selected time interval showing the details of weak hydrogen bond breakage by water and strong hydrogen bond recombination (MP4)

AUTHOR INFORMATION

Corresponding Authors

Lifeng Chi − *Institute of Functional Nano & Soft Materials (FUNSOM), Jiangsu Key Laboratory for Carbon-Based Functional Materials and Devices, Joint International Research Laboratory of Carbon-Based Functional Materials and Devices, Soochow University, Suzhou 215123, China;* ⓘ orcid.org/0000-0003-3835-2776; Email: chilf@suda.edu.cn

Xiaohui Qiu − *CAS Key Laboratory of Standardization and Measurement for Nanotechnology, CAS Center for Excellence in Nanoscience, National Center for Nanoscience and Technology, Beijing 100190, China; University of Chinese Academy of Sciences, Beijing 100049, China;* Email: xhqiu@nanoctr.cn

Wei Xu − *Interdisciplinary Materials Research Center, College of Materials Science and Engineering, Tongji University, Shanghai 201804, China;* ⓘ orcid.org/0000-0003-0216-794X; Email: xuwei@tongji.edu.cn

Authors

Lei Xie − *Interdisciplinary Materials Research Center, College of Materials Science and Engineering, Tongji University, Shanghai 201804, China*

Huijun Jiang − *Hefei National Laboratory for Physical Sciences at the Microscale & Department of Chemical Physics, iChEM, University of Science and Technology of China, Hefei, Anhui 230026, China;* orcid.org/0000-0001-7243-5431

Donglin Li − *Interdisciplinary Materials Research Center, College of Materials Science and Engineering, Tongji University, Shanghai 201804, China*

Mengxi Liu − *CAS Key Laboratory of Standardization and Measurement for Nanotechnology, CAS Center for Excellence in Nanoscience, National Center for Nanoscience and Technology, Beijing 100190, China;* orcid.org/0000-0001-7009-5269

Yuanqi Ding − *Interdisciplinary Materials Research Center, College of Materials Science and Engineering, Tongji University, Shanghai 201804, China*

Yufang Liu − *College of Physics and Materials Science, Henan Normal University, Xinxiang 453007, China*

Xin Li − *CAS Key Laboratory of Standardization and Measurement for Nanotechnology, CAS Center for Excellence in Nanoscience, National Center for Nanoscience and Technology, Beijing 100190, China; University of Chinese Academy of Sciences, Beijing 100049, China*

Xuechao Li − *Institute of Functional Nano & Soft Materials (FUNSOM), Jiangsu Key Laboratory for Carbon-Based Functional Materials and Devices, Joint International Research Laboratory of Carbon-Based Functional Materials and Devices, Soochow University, Suzhou 215123, China*

Haiming Zhang − *Institute of Functional Nano & Soft Materials (FUNSOM), Jiangsu Key Laboratory for Carbon-Based Functional Materials and Devices, Joint International Research Laboratory of Carbon-Based Functional Materials and Devices, Soochow University, Suzhou 215123, China;* orcid.org/0000-0001-5986-5314

Zhonghuai Hou − *Hefei National Laboratory for Physical Sciences at the Microscale & Department of Chemical Physics, iChEM, University of Science and Technology of China, Hefei, Anhui 230026, China;* orcid.org/0000-0003-1241-7041

Yi Luo − *Hefei National Laboratory for Physical Sciences at the Microscale & Department of Chemical Physics, iChEM, University of Science and Technology of China, Hefei, Anhui 230026, China*

Complete contact information is available at:
https://pubs.acs.org/10.1021/acsnano.0c05227

Author Contributions

▽L.X., H.J., D.L., and M.L. contributed equally to this work.

Notes

The authors declare no competing financial interest.

REFERENCES

(1) Whitesides, G. M.; Mathias, J. P.; Seto, C. T. Molecular Self-Assembly and Nanochemistry: A Chemical Strategy for the Synthesis of Nanostructures. *Science* **1991**, *254*, 1312−1319.

(2) Philp, D.; Stoddart, J. F. Self-Assembly in Natural and Unnatural Systems. *Angew. Chem., Int. Ed. Engl.* **1996**, *35*, 1154−1196.

(3) Černý, J.; Hobza, P. Non-Covalent Interactions in Biomacromolecules. *Phys. Chem. Chem. Phys.* **2007**, *9*, 5291−5303.

(4) Kilchherr, F.; Wachauf, C.; Pelz, B.; Rief, M.; Zacharias, M.; Dietz, H. Single-Molecule Dissection of Stacking Forces in DNA. *Science* **2016**, *353*, aaf5508.

(5) Johannsen, S.; Megger, N.; Böhme, D.; Sigel, R. K. O.; Müller, J. Solution Structure of a DNA Double Helix with Consecutive Metal-Mediated Base Pairs. *Nat. Chem.* **2010**, *2*, 229−234.

(6) Takezawa, Y.; Mitsuhiko, S. Metal-Mediated DNA Base Pairing: Alternatives to Hydrogen-Bonded Watson−Crick Base Pairs. *Acc. Chem. Res.* **2012**, *45*, 2066−2076.

(7) Zhou, H.-X.; Pang, X. Electrostatic Interactions in Protein Structure, Folding, Binding, and Condensation. *Chem. Rev.* **2018**, *118*, 1691−1741.

(8) Bishop, K. J.; Wilmer, C. E.; Soh, S.; Grzybowski, B. A. Nanoscale Forces and Their Uses in Self-Assembly. *Small* **2009**, *5*, 1600−1630.

(9) Laage, D.; Elsaesser, T.; Hynes, J. T. Water Dynamics in the Hydration Shells of Biomolecules. *Chem. Rev.* **2017**, *117*, 10694−10725.

(10) Nandi, N.; Bhattacharyya, K.; Bagchi, B. Dielectric Relaxation and Solvation Dynamics of Water in Complex Chemical and Biological Systems. *Chem. Rev.* **2000**, *100*, 2013−2046.

(11) Schiebel, J.; Gaspari, R.; Wulsdorf, T.; Ngo, K.; Sohn, C.; Schrader, T. E.; Cavalli, A.; Ostermann, A.; Heine, A.; Klebe, G. Intriguing Role of Water in Protein-Ligand Binding Studied by Neutron Crystallography on Trypsin Complexes. *Nat. Commun.* **2018**, *9*, 3559.

(12) Nagornova, N. S.; Rizzo, T. R.; Boyarkin, O. V. Interplay of Intra- and Intermolecular H-Bonding in a Progressively Solvated Macrocyclic Peptide. *Science* **2012**, *336*, 320−323.

(13) Lucht, K.; Loose, D.; Ruschmeier, M.; Strotkötter, V.; Dyker, G.; Morgenstern, K. Hydrophilicity and Microsolvation of an Organic Molecule Resolved on the Sub-Molecular Level by Scanning Tunneling Microscopy. *Angew. Chem., Int. Ed.* **2018**, *57*, 1266−1270.

(14) Henzl, J.; Boom, K.; Morgenstern, K. Using the First Steps of Hydration for the Determination of Molecular Conformation of a Single Molecule. *J. Am. Chem. Soc.* **2014**, *136*, 13341−13347.

(15) Zhang, C.; Xie, L.; Ding, Y.; Xu, W. Scission and Stitching of Adenine Structures by Water Molecules. *Chem. Commun.* **2018**, *54*, 771−774.

(16) Otero, R.; Lukas, M.; Kelly, R. E. A.; Xu, W.; Lægsgaard, E.; Stensgaard, I.; Kantorovich, L. N.; Besenbacher, F. Elementary Structural Motifs in a Random Network of Cytosine Adsorbed on a Gold(111) Surface. *Science* **2008**, *319*, 312−315.

(17) Kong, H.; Wang, L.; Sun, Q.; Zhang, C.; Tan, Q.; Xu, W. Controllable Scission and Seamless Stitching of Metal-Organic Clusters by STM Manipulation. *Angew. Chem., Int. Ed.* **2015**, *54*, 6526−6530.

(18) Zhang, C.; Xie, L.; Wang, L.; Kong, H.; Tan, Q.; Xu, W. Atomic-Scale Insight into Tautomeric Recognition, Separation and Interconversion of Guanine Molecular Networks on Au(111). *J. Am. Chem. Soc.* **2015**, *137*, 11795−11800.

(19) Kong, H.; Sun, Q.; Wang, L.; Tan, Q.; Zhang, C.; Sheng, K.; Xu, W. Atomic-Scale Investigation on the Facilitation and Inhibition of Guanine Tautomerization at Au(111) Surface. *ACS Nano* **2014**, *8*, 1804−1808.

(20) Papageorgiou, A. C.; Fischer, S.; Reichert, J.; Diller, K.; Blobner, F.; Klappenberger, F.; Allegretti, F.; Seitsonen, A. P.; Barth, J. V. Chemical Transformations Drive Complex Self-Assembly of Uracil on Close-Packed Coinage Metal Surfaces. *ACS Nano* **2012**, *6*, 2477−2486.

(21) Shukla, M. K.; Leszczynski, J. Interaction of Water Molecules with Cytosine Tautomers: An Excited-State Quantum Chemical Investigation. *J. Phys. Chem. A* **2002**, *106*, 11338−11346.

(22) Feyer, V.; Plekan, O.; Richter, R.; Coreno, M.; Vall-llosera, G.; Prince, K. C.; Trofimov, A. B.; Zaytseva, I. L.; Moskovskaya, T. E.; Gromov, E. V.; Schirmer, J. Tautomerism in Cytosine and Uracil: An Experimental and Theoretical Core Level Spectroscopic Study. *J. Phys. Chem. A* **2009**, *113*, 5736−5742.

(23) Liu, R. Adsorption and Dissociation of H_2O on Au(111) Surface: A DFT Study. *Comput. Theor. Chem.* **2013**, *1019*, 141−145.

(24) Peng, J.; Guo, J.; Ma, R.; Meng, X.; Jiang, Y. Atomic-Scale Imaging of the Dissolution of NaCl Islands by Water at Low Temperature. *J. Phys.: Condens. Matter* **2017**, *29*, 104001.

(25) Besenbacher, F. Scanning Tunneling Microscopy Studies of Metal Surfaces. *Rep. Prog. Phys.* **1996**, *59*, 1737.

(26) Lægsgaard, E.; Österlund, L.; Thostrup, P.; Rasmussen, P. B.; Stensgaard, I.; Besenbacher, F. A High-Pressure Scanning Tunneling Microscope. *Rev. Sci. Instrum.* **2001**, *72*, 3537−3542.

(27) Chen, J.; Guo, J.; Meng, X.; Peng, J.; Sheng, J.; Xu, L.; Jiang, Y.; Li, X.-Z.; Wang, E.-G. An Unconventional Bilayer Ice Structure on a NaCl(001) Film. *Nat. Commun.* **2014**, *5*, 4056.

(28) Kresse, G.; Hafner, J. *Ab Initio* Molecular Dynamics for Open-Shell Transition Metals. *Phys. Rev. B: Condens. Matter Mater. Phys.* **1993**, *48*, 13115−13118.

(29) Kresse, G.; Furthmüller, J. Efficient Iterative Schemes for *Ab Initio* Total-Energy Calculations Using a Plane-Wave Basis Set. *Phys. Rev. B: Condens. Matter Mater. Phys.* **1996**, *54*, 11169−11186.

(30) Blöchl, P. E. Projector Augmented-Wave Method. *Phys. Rev. B: Condens. Matter Mater. Phys.* **1994**, *50*, 17953−17979.

(31) Kresse, G.; Joubert, D. From Ultrasoft Pseudopotentials to the Projector Augmented-Wave Method. *Phys. Rev. B: Condens. Matter Mater. Phys.* **1999**, *59*, 1758−1775.

(32) Perdew, J. P.; Burke, K.; Ernzerhof, M. Generalized Gradient Approximation Made Simple. *Phys. Rev. Lett.* **1996**, *77*, 3865.

(33) Grimme, S.; Antony, J.; Ehrlich, S.; Krieg, H. A Consistent and Accurate *Ab Initio* Parametrization of Density Functional Dispersion Correction (DFT-D) for the 94 Elements H-Pu. *J. Chem. Phys.* **2010**, *132*, 154104.

(34) Frisch, M. J.; Trucks, G. W.; Schlegel, H. B.; Scuseria, G. E.; Robb, M. A.; Cheeseman, J. R.; Scalmani, G.; Barone, V.; Petersson, G. A.; Nakatsuji, H.; Li, X.; Caricato, M.; Marenich, A. V.; Bloino, J.; Janesko, B. G.; Gomperts, R.; Mennucci, B.; Hratchian, H. P.; Ortiz, J. V.; Izmaylov, A. F.; et al. *Gaussian 16*, Revision B.01; Gaussian, Inc.: Wallingford, CT, 2016.

(35) Sen, K.; Crespo-Otero, R.; Weingart, O.; Thiel, W.; Barbatti, M. Interfacial States in Donor-Acceptor Organic Heterojunctions: Computational Insights into Thiophene-Oligomer/Fullerene Junctions. *J. Chem. Theory Comput.* **2013**, *9*, 533−542.

(36) Frisch, M. J.; Pople, J. A.; Binkley, J. S. Self-Consistent Molecular Orbital Methods 25. Supplementary Functions for Gaussian Basis Sets. *J. Chem. Phys.* **1984**, *80*, 3265−3269.

(37) Lu, T.; Chen, F. Multiwfn: A Multifunctional Wavefunction Analyzer. *J. Comput. Chem.* **2012**, *33*, 580−592.

(38) Kelly, R. E. A.; Lee, Y. J.; Kantorovich, L. N. Homopairing Possibilities of the DNA Bases Cytosine and Guanine: An *Ab Initio* DFT Study. *J. Phys. Chem. B* **2005**, *109*, 22045−22052.

(39) Lippincott, E. R.; Schroeder, R. One-Dimensional Model of the Hydrogen Bond. *J. Chem. Phys.* **1955**, *23*, 1099−1106.

(40) Stillinger, F. H.; Rahman, A. Improved Simulation of Liquid Water by Molecular Dynamics. *J. Chem. Phys.* **1974**, *60*, 1545−1557.

(41) Giguère, P. A. The Bifurcated Hydrogen-Bond Model of Water and Amorphous Ice. *J. Chem. Phys.* **1987**, *87*, 4835−4839.